Proceedings of the XVI National Conference on Superconductivity and Strongly Correlated Systems, Zakopane 2013

Resonant Two-Electron Pairs in a Simple Cubic Lattice

M. Bak*

Faculty of Physics, A. Mickiewicz University, Umultowska 85, 61-614 Poznań, Poland

The properties of resonant two-electron pairs are examined in three-dimensional simple cubic extended Hubbard tUW model, in s- and d- symmetry channels, in the limit of empty lattice. Lattice Green function technique is applied to calculate the scattering amplitude by means of $\mathcal{T}$ matrix for any energy in the band on ΓR line within the Brillouin zone. The analysis shows the persistence of resonant states even for Coulomb interactions so weak that the equation for the resonant states is not formally fulfilled. The difference in behavior of resonances controlled by on-site and intersite Coulomb interactions is found. The ranges of applicability of approximate formula for the actual position of resonant peak and its width are shown.

DOI: 10.12693/APhysPolA.126.A-63

PACS: 71.10.Fd, 31.15.xh, 71.10.Li, 71.55.–i, 03.65.Ge, 02.30.Zz

1. Introduction

The pairing gap in superconducting cuprates, which is the most intensively researched family of high-temperature superconductors (HTS), is of the d-wave symmetry [1]. It is believed that the superconductivity in those materials is of quasi-two-dimensional nature. There are also other groups of materials, with different properties, usually with lower critical temperature, which are nevertheless believed to have similar, unconventional mechanism of superconductivity (probably connected with strong electron correlations) [2]. The examples are three-dimensional (3D) Chevrel phases [3] or doped $BaBiO_3$, ruthenates with triplet p-wave pairing [4], 3D heavy fermion materials [5], borocarbides with extended s or $s+g$ three-dimensional symmetry [6], topological insulators, insulating in the bulk and $p_x + \mathrm{i}p_y$-wave on the surface [7], pnictides with possible $s_{\pm}$-wave pairing [8] and dimensional crossover 3D–2D [9]. A very interesting is also the normal phase of HTS, which often exhibits pseudogap [10]. A basic ingredient of all these phenomena is a two-electron or two-hole pair, with either large (Cooper pair) or small (local pair) radius. Transition between those two regimes is known as BCS–BEC transition, a very interesting and difficult problem [11–15]. The properties of a single pair seem perfectly suited to probe this subject, though we must remember that the properties of a pair usually do not have a simple and direct translation into the properties of superconducting state [16]. Nevertheless, the problem of two particles on a lattice is a very interesting one and it is also one of few examples in solid state physics, which enjoy an exact solution (in the empty lattice limit). The pair's properties are especially important in the context of negative-U Hubbard model or boson-fermion model of superconductivity [17], where bound and resonant states appear naturally.

While the behavior of bound pairs in 2D is known [15, 18–32], the problem in 3D was given less attention. Three-dimensional bound pairs of magnons were subject of intensive research in sixties [33, 34] but then the development was hampered by mathematical difficulties in calculating 3D lattice Green function (LGF), especially concerning the resonant states, expressed by singular integrals. In seventies Joyce [35] found an analytical expression for 3D LGF's but by then the interest in the subject diminished. In view of the fundamental role played in the field of superconductivity by two-particle states and unclear importance of the third dimension, as described in preceding paragraph, the author considers it worthwhile to examine the properties of bound and particularly resonant states in 3D, with the special emphasis on the behavior within the symmetry channels. One further argument in favor of such analysis is the probability of practical realization of these states in optical lattices in the close future. The 1D bosonic states' properties have already been thoroughly analyzed [36, 37], the 3D states only await small technological progress.

To perform the current analysis the lattice Green function approach will be used [38, 39], which will turn equivalent to the well known impurity problem on a lattice in a subspace of fixed total momentum of a pair [40]; the symmetry transformations for the states within the distance of the Coulomb interaction of the model will be applied [40, 41]. We shall consider the extended Hubbard model, which naturally admits other than s-wave pairings, in particular the most widespread d-wave type.

The plan of work is as follows: after Introduction the formalism will be sketched in Sect. 2, where the reduction to the problem of one impurity on a lattice will be shown. The properties of resonant states in various symmetry channels will be described in Sect. 3 and the paper will be closed by Conclusions.

2. Formalism

2.1. The Hamiltonian and its eigenstates

The Hamiltonian is given by $H = H_0 + H_{\mathrm{I}}$, with

$$H_0 = \sum_{\langle i,j \rangle} t_{i,j} c_i^{\dagger} c_j, \tag{1}$$

*e-mail: mbak@amu.edu.pl

$$H_{\rm I} = U\sum_i n_{i,\uparrow}n_{i,\downarrow} + \frac{W}{2}\sum_{\langle i,j\rangle}\sum_{\sigma,\sigma'} n_{i,\sigma}n_{j,\sigma'}, \quad (2)$$

where t_{ij} is the hopping integral and $c^\dagger_{i,\sigma}$ creates a Wannier state at a site i.

The two-particle eigenstates of H_0 have fixed momenta $\boldsymbol{k}_1$ and $\boldsymbol{k}_2$ of particles, which can also be described by center of mass $\boldsymbol{K} = \boldsymbol{k}_1 + \boldsymbol{k}_2$ and relative $\boldsymbol{k} = (\boldsymbol{k}_2 - \boldsymbol{k}_1)/2$ momenta

$$H_0|\boldsymbol{K},\boldsymbol{k},\sigma_1,\sigma_2\rangle = E_{\boldsymbol{K},\boldsymbol{k}}|\boldsymbol{K},\boldsymbol{k},\sigma_1,\sigma_2\rangle, \quad (3)$$

$$|\boldsymbol{K},\boldsymbol{k},\sigma_1,\sigma_2\rangle = |\boldsymbol{k}_1\sigma_1,\boldsymbol{k}_2\sigma_2\rangle = c^\dagger_{\boldsymbol{k}1,\sigma 1}c^\dagger_{\boldsymbol{k}2,\sigma 2}|0\rangle, \quad (4)$$

$$E_{\boldsymbol{K},\boldsymbol{k}} = \epsilon_{\boldsymbol{K}+\boldsymbol{k}/2} + \epsilon_{\boldsymbol{K}-\boldsymbol{k}/2} = \epsilon_{\boldsymbol{k}1} + \epsilon_{\boldsymbol{k}2}, \quad (5)$$

where $c^\dagger_{\boldsymbol{k},\sigma}$ creates Bloch state with quasimomentum $\boldsymbol{k}$ and spin σ, $-t = t_{i,j}$ and $\epsilon_{\boldsymbol{k}} = \sum_{\boldsymbol{\delta}} t(\boldsymbol{\delta})\exp(\mathrm{i}\boldsymbol{k}\boldsymbol{\delta})$, where $\boldsymbol{\delta}$ connects nearest neighbors (nn). The eigenenergy in the specific case of simple cubic lattice

$$E^{sc}_{\boldsymbol{K},\boldsymbol{k}} = -4t\left(\cos\frac{\boldsymbol{K}_x}{2}\cos\boldsymbol{k}_x a_x + \cos\frac{\boldsymbol{K}_y}{2}\cos\boldsymbol{k}_y a_y + \alpha\cos\frac{\boldsymbol{K}_z}{2}\cos\boldsymbol{k}_z a_z\right), \quad (6)$$

where a_x, a_y, a_z are lattice constants and α is possible z-axis anisotropy parameter.

On the other hand, $H_{\rm I}$ is diagonal within the local orbitals basis $|\boldsymbol{i}\sigma_1,\boldsymbol{j}\sigma_2\rangle = c^\dagger_{\boldsymbol{i}\sigma_1}c^\dagger_{\boldsymbol{j}\sigma_2}|0\rangle$, where $c^\dagger_{\boldsymbol{i}\sigma}$ creates a Wannier state centered around site $\boldsymbol{i}$ of a lattice. As we assume periodic boundary conditions, the system is translationally invariant and this means that the center-of-mass' (quasi)momentum $\boldsymbol{K}$ is conserved quantity. Thus it is useful to transform local basis vectors into the relative: $\boldsymbol{r} = \boldsymbol{i} - \boldsymbol{j}$ and center-of-mass: $\boldsymbol{R}_{\rm cm} = (\boldsymbol{i} + \boldsymbol{j})/2$ (which couples to $\boldsymbol{K}$) coordinates — we create "mixed" basis

$$|\boldsymbol{K},\boldsymbol{r},\sigma_1,\sigma_2\rangle = \frac{1}{\sqrt{N}}\sum_{\boldsymbol{r}'}\exp\left(\mathrm{i}\boldsymbol{K}\cdot(\boldsymbol{r}'+\boldsymbol{r}/2)\right)c^\dagger_{\boldsymbol{r}',\sigma 1}c^\dagger_{\boldsymbol{r}'+\boldsymbol{r},\sigma 2}|0\rangle, \quad (7)$$

where N is number of lattice sites. Mixed basis is orthogonal

$$\langle\boldsymbol{K},\boldsymbol{r},\sigma_1,\sigma_2|\boldsymbol{K}',\boldsymbol{r}',\sigma_1',\sigma_2'\rangle = \delta_{\boldsymbol{K},\boldsymbol{K}'}(\delta_{\boldsymbol{r},\boldsymbol{r}'}\delta_{\sigma 1,\sigma 1'}\delta_{\sigma 2,\sigma 2'} - \delta_{\boldsymbol{r},-\boldsymbol{r}'}\delta_{\sigma 1,\sigma 2'}\delta_{\sigma 2,\sigma 1'}), \quad (8)$$

and its overlap with the momentum basis consists of plane waves

$$\langle\boldsymbol{K},\boldsymbol{r},\sigma_1,\sigma_2|\boldsymbol{K}',\boldsymbol{k},\sigma_1',\sigma_2'\rangle = \frac{\delta_{\boldsymbol{K},\boldsymbol{K}'}}{\sqrt{N}}\left(\mathrm{e}^{\mathrm{i}\boldsymbol{k}\boldsymbol{r}}\delta_{\sigma 1,\sigma 1'}\delta_{\sigma 2,\sigma 2'} - \mathrm{e}^{-\mathrm{i}\boldsymbol{k}\boldsymbol{r}}\delta_{\sigma 1,\sigma 2'}\delta_{\sigma 2,\sigma 1'}\right). \quad (9)$$

$H_{\rm I}$ is diagonal in mixed basis

$$\langle\boldsymbol{K},\boldsymbol{r},\uparrow,\downarrow|H_{\rm I}|\boldsymbol{K}',\boldsymbol{r}',\uparrow,\downarrow\rangle = \delta_{\boldsymbol{K},\boldsymbol{K}'}\delta_{\boldsymbol{r}',\boldsymbol{r}}\left(U\delta_{\boldsymbol{r},0} + W\delta_{\boldsymbol{r},\boldsymbol{\delta}}\right) \quad (10)$$

(while only W part for both same spins) while

$$H_0|\boldsymbol{K},\boldsymbol{r},\sigma_1,\sigma_2\rangle = \sum_{\boldsymbol{\delta}} 2t(\boldsymbol{\delta})\cos(\boldsymbol{K}\cdot\boldsymbol{\delta}/2)|\boldsymbol{K},\boldsymbol{r}+\boldsymbol{\delta},\sigma_1,\sigma_2\rangle. \quad (11)$$

As we see, the Hamiltonian leaves the center of mass momentum $\boldsymbol{K}$ unchanged. For fixed $\boldsymbol{K}$ Eq. (11) describes the hopping of *one* particle on the lattice spanned by the relative position vectors $\boldsymbol{r}$. The latter is the same as the crystal lattice, with the difference that on the "relative" lattice one site — the central one — is distinguished. Thus the problem is equivalent to single impurity problem on a lattice and we may further apply the existing theory of that phenomenon [38, 40, 41].

2.2. Resonant states

The solution of Schrödinger equation

$$(H_0 + H_{\rm I})|\psi\rangle = E|\psi\rangle, \quad (12)$$

can be formally expressed as

$$|\psi\rangle = G_0 H_{\rm I}|\psi\rangle, \quad (13)$$

$$G_0 = (E - H_0)^{-1} = \sum_{\boldsymbol{k}}\frac{|\boldsymbol{k}\rangle\langle\boldsymbol{k}|}{E - E_{\boldsymbol{k}}}, \quad (14)$$

where G_0 is Green function and $H_0|\boldsymbol{k}\rangle = E_{\boldsymbol{k}}|\boldsymbol{k}\rangle$. Within the subspace of fixed $\boldsymbol{K}$, $|\boldsymbol{k}\rangle$'s are given by (4) and $E_{\boldsymbol{k}}$ by (6). $E_{\boldsymbol{k}}$'s for all possible values of $\boldsymbol{k}$ create an energetic band; solution of Eq. (13) may exist for specific energies E (dependent on parameters of $H_{\rm I}$) *outside* the band — the energies of bound states, corresponding to well defined G_0. This E is calculated from the condition on non-trivial solutions of homogeneous Eq. (13):

$$\det(I - G_0 H_{\rm I}) = 0. \quad (15)$$

E may also lay within the band — we speak then about resonant state with singular G_0. The singularity is dealt with in a standard way, by adding small infinitesimal imaginary part to the energy, changing G_0 into G_0^+.

2.2.1. Lippmann–Schwinger equation

Usually the equation for resonant states includes also the wave function of incident particle and is called the Lippmann–Schwinger equation then

$$|\psi\rangle = |\boldsymbol{q}\rangle + G_0^+(E,\boldsymbol{K})H_{\rm I}|\psi\rangle, \quad (16)$$

where $|\boldsymbol{q}\rangle$ describes incident particle with the wave vector $\boldsymbol{q}$. Formal solution of (16) reads

$$|\psi\rangle = (I - G_0^+ H_{\rm I})^{-1}|\boldsymbol{q}\rangle, \quad (17)$$

which can be substituted back onto the right hand side (r.h.s.) of (16) to obtain

$$|\psi\rangle = |\boldsymbol{q}\rangle + G_0^+(E,\boldsymbol{K})H_{\rm I}(I - G_0^+ H_{\rm I})^{-1}|\boldsymbol{q}\rangle = |\boldsymbol{q}\rangle + G_0^+(E,\boldsymbol{K})\mathcal{T}^+|\boldsymbol{q}\rangle, \quad (18)$$

where we used the fact that $(I - G_0^+ H_{\rm I})^{-1} = H_{\rm I}^{-1}(H_{\rm I}^{-1} - G_0^+)^{-1}$ and introduced the $\mathcal{T}$-matrix: $\mathcal{T}^+ = \left(\boldsymbol{V}^{-1} - \boldsymbol{G}_0^+(E,\boldsymbol{K})\right)^{-1}$. The wave function, Eq. (13) can be expanded in any complete orthonormal set of states $|\boldsymbol{r}\rangle$:

$$\langle\boldsymbol{r}|\psi\rangle = \langle\boldsymbol{r}|\boldsymbol{q}\rangle + \sum_{\boldsymbol{r}'}\sum_{\boldsymbol{r}''}\langle\boldsymbol{r}|G_0^+|\boldsymbol{r}'\rangle\langle\boldsymbol{r}'|\mathcal{T}^+|\boldsymbol{r}''\rangle\langle\boldsymbol{r}''|\boldsymbol{q}\rangle. \quad (19)$$

2.2.2. Koster–Slater improvement

The most important notion of the theory is that if $|\boldsymbol{r}\rangle$'s describe localized states, and we arrange the basis,

so that the small $\boldsymbol{r}$'s, close to the lattice origin (denoted by capital $\boldsymbol{R}$ henceforth), are gathered in the beginning of the basis set, then H_{I} in that basis acquires block diagonal form [38]:

$$H_{\mathrm{I}} = \begin{pmatrix} \boldsymbol{V} & 0 \\ 0 & 0 \end{pmatrix}, \tag{20}$$

where $\boldsymbol{V}$ is diagonal matrix with elements $\langle \boldsymbol{r}|H_{\mathrm{I}}|\boldsymbol{r}\rangle$ given by (10). The size of $\boldsymbol{V}$ is equal to the number of sites connected by the Coulomb interactions to the site "0". It determines the size of the system of equations to be solved, so changing to the local basis is a great progress compared to the momentum basis (4), where one needs as many basis vectors (and equations) as there are lattice sites.

A good choice of basis $|\boldsymbol{r}\rangle$ is "mixed" states basis (7). If we define a vector consisting of the wave functions on the "close" sites, i.e., the largest vector which can be changed by $\boldsymbol{V}$, then the whole vector of wave functions can be calculated from the matrix equation looking exactly like Eq. (18), where by $|\psi\rangle$ we mean the vector of wave functions $\langle \boldsymbol{R}|\psi\rangle$, by $|\boldsymbol{q}\rangle$ a vector consisting of plane waves on close sites $\langle \boldsymbol{R}|\boldsymbol{q}\rangle$, by G_0^+ a matrix in position representation and $\mathcal{T}^+$ is a matrix with elements defined by:

$$\langle \boldsymbol{R}|(\mathcal{T}^+)^{-1}|\boldsymbol{R}'\rangle = \langle \boldsymbol{R}|\boldsymbol{V}^{-1}|\boldsymbol{R}'\rangle - \langle \boldsymbol{R}|\boldsymbol{G}_0^+|\boldsymbol{R}'\rangle. \tag{21}$$

When $|\psi\rangle$, i.e., $\langle \boldsymbol{R}|\psi\rangle$ for all "close" $\boldsymbol{R}$'s are known, Eq. (19), with $\sum_{\boldsymbol{r},\boldsymbol{r}'}$ changed into $\sum_{\boldsymbol{R},\boldsymbol{R}'}$, can be used to calculate the wave functions on "far" sites $\langle \boldsymbol{r}|\psi\rangle$.

2.2.3. Symmetry basis

We can further simplify matters by applying unitary transformation to the wave functions on "close" sites and create their linear combinations transforming according to irreducible representations (irreps) of the point symmetry group of a lattice [41]. Such combinations consist of $\boldsymbol{R}$'s, which are transformed into one another by the operations of the point group, i.e., of $\boldsymbol{R}$'s of the same length $|\boldsymbol{R}|$ within group theoretic *star* of $\boldsymbol{R}$. Thus the symmetric combinations are made within the "layers" of the same $|\boldsymbol{R}| = R$, so the new, symmetric basis is denoted as $|x_R\rangle$, where x signifies an irrep and the length R — the layer. In case of longer ranged Coulomb interactions more indices can be added

$$\langle \boldsymbol{r}|\psi\rangle = \langle \boldsymbol{r}|\boldsymbol{q}\rangle + \sum_x \sum_{R,R'} \langle \boldsymbol{r}|\boldsymbol{G}_0^+(E,\boldsymbol{K})|x_R\rangle\langle x_R|\mathcal{T}^+|x_R\rangle\langle x_{R'}|\boldsymbol{q}\rangle, \tag{22}$$

$$\langle x_R|\mathcal{T}^+|x_{R'}\rangle = \sum_{\boldsymbol{R},\boldsymbol{R}'} U_{x,\boldsymbol{R}}\mathcal{T}^+_{\boldsymbol{R},\boldsymbol{R}'}U^\dagger_{\boldsymbol{R}',x} = \sum_{\boldsymbol{R},\boldsymbol{R}'} \langle x_R|\boldsymbol{R}\rangle((\mathcal{T}^+)^{-1}_{\boldsymbol{R},\boldsymbol{R}'})^{-1}\langle \boldsymbol{R}'|x_{R'}\rangle, \tag{23}$$

where U denotes unitary transformation matrix consisting of elements $\langle x_R|\boldsymbol{R}\rangle$ and $\langle x_R|\boldsymbol{q}\rangle$ which are linear combinations of plane waves on "close" sites transforming according to irreducible representations of lattice point group, created by the same transformation $\langle x_R|\boldsymbol{q}\rangle = (U|\boldsymbol{q}\rangle)_x = \sum_{\boldsymbol{R}\in R}\langle x_R|\boldsymbol{R}\rangle\langle \boldsymbol{R}|\boldsymbol{q}\rangle$.

In the symmetric basis the $\mathcal{T}^+$-matrix becomes block diagonal. For a general $\boldsymbol{K}$ the singlets get separated from the triplets, while for $\boldsymbol{K}$ on some symmetry line further blocking is possible. The maximal separation into symmetry channels is for $\boldsymbol{K} = 0$ (and on simple cubic lattice for $\boldsymbol{K}$ on ΓR line — on the main diagonal).

For the simple cubic lattice with lattice constants $a_x = R_x$, $a_y = R_y$, $a_z = R_z$, we have the following nonzero U-matrix elements: $\langle x_R|\boldsymbol{R}\rangle$ [41, 43]: $\langle s_0|R_0\rangle = 1$, $\langle s_1|\boldsymbol{R}_{\pm\xi}\rangle = 1/\sqrt{6}$ for $\xi = x,y,z$, $\langle p_\xi|\boldsymbol{R}_\xi\rangle = -\langle p_\xi|\boldsymbol{R}_{-\xi}\rangle = 1/\sqrt{2}$ for $\xi = x,y,z$, $\langle d_\alpha|\boldsymbol{R}_{\pm z}\rangle = -\langle d_\alpha|\boldsymbol{R}_{\pm y}\rangle = 1/2$, $\langle d_\beta|\boldsymbol{R}_{\pm x}\rangle = 1/\sqrt{3}$ and $\langle d_\beta|\boldsymbol{R}_\xi\rangle = -1/2\sqrt{3}$ for $\xi = \pm y, \pm z$.

$$\begin{aligned}\langle \boldsymbol{q}|U^\dagger = (&\langle \boldsymbol{q}|R_0\rangle, \langle \boldsymbol{q}|R_x\rangle, \langle \boldsymbol{q}|R_{-x}\rangle,\\ &\langle \boldsymbol{q}|R_y\rangle, \langle \boldsymbol{q}|R_{-y}\rangle, \langle \boldsymbol{q}|R_z\rangle, \langle \boldsymbol{q}|R_{-z}\rangle)\, U^\dagger =\\ &(\langle \boldsymbol{q}|s_0\rangle,\langle \boldsymbol{q}|s_1\rangle,\langle \boldsymbol{q}|p_x\rangle,\langle \boldsymbol{q}|p_y\rangle, \langle \boldsymbol{q}|p_z\rangle,\langle \boldsymbol{q}|d_\alpha\rangle,\langle \boldsymbol{q}|d_\beta\rangle) =\\ &\Big(1, \sqrt{2/3}(\cos q_x + \cos q_y + \cos q_z), \mathrm{i}\sqrt{2}\sin q_x,\\ &\mathrm{i}\sqrt{2}\sin q_y, \mathrm{i}\sqrt{2}\sin q_z, \cos q_y - \cos q_z,\\ &(2\cos q_x - \cos q_y - \cos q_z)/\sqrt{3}\Big),\end{aligned} \tag{24}$$

where $d_\alpha = d_{y^2-z^2}$, $d_\beta = d_{2x^2-y^2-z^2}$ and in the last equation we assumed $a_x = a_y = a_z = 1$.

2.2.4. Scattering amplitude

It can be proved that for large $\boldsymbol{r}$, $\langle \boldsymbol{r}|\boldsymbol{G}_0^+|x_R\rangle$ becomes proportional to the spherical wave [40]:

$$(\boldsymbol{G}_0^+)_{x,r\to\infty} \longrightarrow \mathrm{const}\frac{\exp(\mathrm{i}\boldsymbol{q}_0\boldsymbol{r})}{|\boldsymbol{r}|}, \tag{25}$$

where $\boldsymbol{q}_0$ is certain special wave vector. Thus the multiplier of $\boldsymbol{G}_0^+$ in Eq. (22) is by definition proportional to the scattering amplitude f, so

$$f \sim \mathcal{T}^+(E). \tag{26}$$

The total cross-section is defined in the usual way as $\sigma_D = |f|^2$. The constant in Eq. (25) is nonsingular, so the $\mathcal{T}$ matrix is mostly responsible for the maxima of f. In the following I will calculate *normalized* $\mathcal{T}^+$, so the contribution of the constant will be unimportant and we can consider f as proportional to $\mathcal{T}^+$. In particular possible peaks of $\mathcal{T}^+$ matrix will correspond to the peaks of σ_D, i.e., to the resonant states.

Let us note that Eq. (22) expresses the scattering amplitude as a sum of contributions from the irreps of the symmetry group of a potential and is therefore an analog of the usual partial-wave formula. Equation (22) finds solutions for any E within the band and so the different symmetry channels do not decouple, as is the case with the bound states. Nevertheless, as, in general, the resonance peaks will appear for different energies in different symmetry channels we may identify them with symmetry label and examine them separately.

There is a "continuity" between bound and resonant states in the sense that the resonant are "created" from the bound states, which have crossed the band boundary.

There is also a continuity in their mathematical description. The bound states' energies are calculated from the equation $\det(\boldsymbol{V}^{-1} - \boldsymbol{G}_0(E,\boldsymbol{K})) = 0$. When E crosses the band boundary and gets inside the energetic band, G_0 and E become complex. The real part of E is connected with the position of $\mathcal{T}^+$-matrix peak E_r, while its imaginary part — with the peak's width Γ. We obtain them by expanding the following equation (within symmetry blocks) [40], which defines E_0:

$$\det\left(\boldsymbol{V}^{-1} - \mathrm{Re}\left(\boldsymbol{G}_0^+(E_0,\boldsymbol{K})\right)\right) =$$

$$\det \mathrm{Re}((\mathcal{T}^+)^{-1}) = 0, \tag{27}$$

where the determinant factorizes for $\boldsymbol{K}$ on ΓR symmetry line in Brillouin zone (B.z.) into

$$\det(\mathcal{T}(E,\boldsymbol{K})^{-1}) =$$

$$D^{(s_0,s_1)} D^{(p_x)} D^{(p_y)} D^{(p_z)} D^{(d_\alpha)} D^{(d_\beta)}. \tag{28}$$

The subdeterminants $D^{(n)}$ for $n = p_x, p_y, p_x, d_\alpha, d_\beta$ have the form

$$D^{(n)} = \frac{1}{W} - \langle n|G_0^+|n\rangle, \tag{29}$$

$$E_r^{(n)} = E_0 - \frac{D_i^{(n)} D_i^{(n)'}}{|D^{(n)'}|^2}, \tag{30}$$

$$\Gamma^{(n)} = \frac{2D_i^{(n)} D_r^{(n)'}}{|D^{(n)'}|^2}, \tag{31}$$

where prime means the energy derivative and $D_i^{(n)}$ and $D_r^{(n)}$ are the imaginary and the real parts respectively of the block of determinant (27) within n-th symmetry channel [40] and $D^{(s_0,s_1)} = \frac{1}{UW} - \frac{1}{U}\langle s_1|G_0^+|s_1\rangle - \frac{1}{W}\langle s_0|G_0^+|s_0\rangle + \langle s_0|G_0^+|s_0\rangle\langle s_1|G_0^+|s_1\rangle - \langle s_0|G_0^+|s_1\rangle^2$, .

By solving the determinant (27) for various $\boldsymbol{K}$ we can obtain the resonant-states' dispersion relations. The following calculations will concern only the ΓR line in sc lattice. On that line the two d-wave pairings and the three p-wave are degenerate.

2.3. Green functions

To calculate $\mathcal{T}$-matrix in symmetry channels, Eq. (23), one needs $\langle x_R|G_0|x_{R'}\rangle = \sum_{\boldsymbol{k}}\langle x_R|\boldsymbol{k}\rangle\langle\boldsymbol{k}|x_{R'}\rangle/(E - E_{\boldsymbol{K},\boldsymbol{k}})$ and to calculate $\langle\boldsymbol{r}|\psi\rangle$, Eq. (22), also $\langle\boldsymbol{r}|G_0^+|x_{R'}\rangle$. If

$$g_{p,q,s} = \frac{1}{\kappa}\frac{1}{\pi^3}\int_0^\pi \frac{\cos p\phi_1 \cos q\phi_2 \cos s\phi_3}{E/\kappa - \cos\phi_1 - \cos\phi_2 - \alpha\cos\phi_3}$$
$$\times \mathrm{d}\phi_1\,\mathrm{d}\phi_2\,\mathrm{d}\phi_3 = (-\mathrm{i})^{p+q+s+1}$$
$$\times \int_0^\infty \exp(\mathrm{i}tE/\kappa) J_p(t) J_q(t) J_s(\alpha t)\,\mathrm{d}t, \tag{32}$$

where $J_n(t)$ denotes a Bessel function of the first kind of order n and $\kappa = -4t\cos K_x/2$ [39]. Then for $\langle\boldsymbol{r}| = \langle p,q,r| = \langle pR_x\boldsymbol{i} + qR_y\boldsymbol{j} + rR_z\boldsymbol{k}|$ we can find the following matrix elements: $f_x^{(p,q,r)} = \langle p,q,r|G_0^+|x\rangle$: $f_{s_0}^{(p,q,r)} = g_{p,q,r}$, $f_{s_1}^{(p,q,r)} = (g_{p-1,q,r} + g_{p+1,q,r} + g_{p,q-1,r} + g_{p,q+1,r} + g_{p,q,r-1} + g_{p,q,r+1})/\sqrt{6}$, $f_{p_x}^{(p,q,r)} = (g_{p-1,q,r} - g_{p+1,q,r})/\sqrt{2}$, $f_{p_y}^{(p,q,r)} = (g_{p,q-1,r} - g_{p,q+1,r})/\sqrt{2}$, $f_{p_z}^{(p,q,r)} = (g_{p,q,r-1} - g_{p,q,r+1})/\sqrt{2}$, $f_{d_\alpha}^{(p,q,r)} = (g_{p+1,q,r} + g_{p-1,q,r} - g_{p,q+1,r} - g_{p,q-1,r})/2$, $f_{d_\beta}^{(p,q,r)} = (2g_{p,q,r+1} + 2g_{p,q,r-1} - g_{p-1,q,r} - g_{p+1,q,r} - g_{p,q+1,r} - g_{p,q-1,r})/(2\sqrt{3})$.

The fully symmetric $\langle x|G_0^+|x\rangle$ are expressible by the products of elliptic integrals [35, 42], but also can be given by the above formulae, with $f_x^{(0,0,0)}$ denoting $\langle x|G_0^+|x\rangle$ and $g_{p,q,r}$ denoting $\langle p,q,r|G_0^+|x\rangle$ (for $p = q = r = 0$ in the left hand side (l.h.s.)). $\langle s_0|G_0^+|s_1\rangle = \langle 0,0,0|G_0^+|s_1\rangle$.

3. Results

3.1. d-wave

In Fig. 1 the results concerning d-wave pairing are shown. The cross-section of horizontal line $t/W \approx -0.074$ ($W/t = -13.5$) with (real) $\langle d_\alpha|G_0|d_\alpha\rangle$ shows the position of the bound state in agreement with Eq. (15). The bound state is indicated by the vertical line in the figure symbolizing the Dirac delta peak.

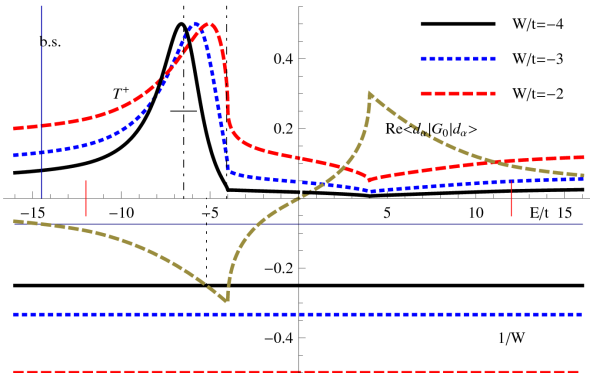

Fig. 1. d-wave: $\mathrm{Re}\langle d_\alpha|G_0|d_\alpha\rangle$, bound state (b.s.), horizontal straight lines are t/W for $W/t = -2, -3, -4, -13.5$ (bottom to top) and $\mathcal{T}^+$-matrices for $W/t = -2$ (dashed), -3 (dotted) and -4 (full line). E_0, E_r and Γ given for $W/t = -2$ by dotted, dot-dashed and horizontal bar respectively. Vertical bars at $E/t = \pm 12$ show extent of the band.

The resonant state connected with $W/t = -4$ appears for energy, which is close to $E_0 \approx -5$, corresponding to the cross-section of $t/W = -0.25$ with the *real* part of G_0 (see Eq. (27)). The approximate energy E_r, Eq. (30), is shown by vertical dot-dashed line. The horizontal bar at half of the height of that line depicts the approximate half width, calculated according to Eq. (31). We see that neither E_r nor Γ are accurate.

The peaks of $\mathcal{T}^+$ move inside the band with decreasing $|W|$ but they do not move past the singularity at $-4\cos(K_x/2)$, which will be called the resonant band boundary.

The horizontal dotted line for $t/W = -0.33$ corresponds to the dotted (positive) plot of $\mathcal{T}^+$-matrix for $W/t = -3$ and analogous pair of dashed lines for $W/t = -2$. Let us note that the absolute value of $|t/W|$ is too large to cross the $\mathrm{Re}(G_0^+)$, because the latter is bounded.

Thus the formal condition for the existence of resonant states, Eq. (27), is *not* fulfilled, but nevertheless the resonant peaks exist and are well defined. Such states will be called quasiresonant. The behavior of the actual

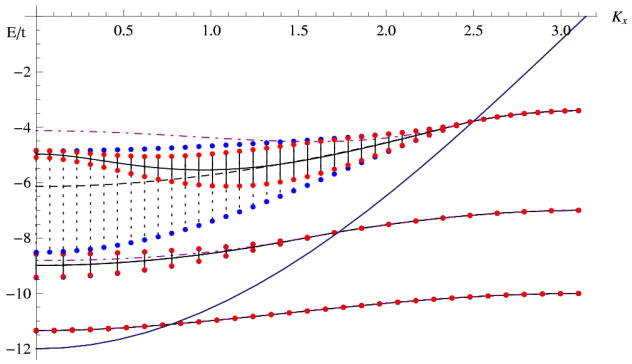

Fig. 2. *d*-wave, actual peak positions (dashed lines), actual half-widths (connected by dotted lines to the peak line), E_r (full lines), Γ (connected by full lines to E_r), E_0 (dot-dashed lines), for $W/t = -10$, -7 and -3.4 (from bottom to top) vs. K_x along ΓR.

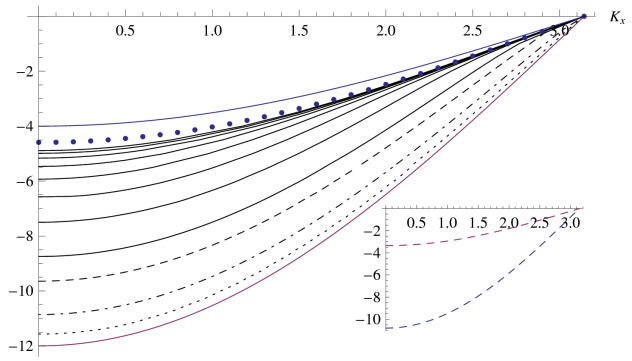

Fig. 3. *d*-wave, actual peak positions of constant half-widths equal to (in "t" units): 0.01, 0.1, 0.5, 1, 2, 3, 4, 5, 6, 7, 8 (from bottom to top) along ΓR. Dots are for half-width bandwidth. Inset: W values described in the text.

scattering cross-section peak for $\boldsymbol{K}$ on ΓR line is shown in Fig. 2 for $W/t = -10$, -7 and -3.4. While for larger $|W|$ the actual peak is quite narrow and narrower than approximate Γ, its width grows monotonously with decreasing $|W|$. It becomes larger than Γ and is quite large when the actual peaks are close to the resonant band boundary. The actual width decreases with increasing K_x, when we approach B.z. boundary. In the same time the energy of the actual peak of $\mathcal{T}^+$-matrix monotonously grows with K_x. This is in contrast with the behavior of E_r and Γ with K_x, which is nonmonotous. Γ can be quite small for small $|W|$ at $K_x = 0$ in contrast with the real width, which is the broadest at $\boldsymbol{K} = 0$ and diminishes to the point at the band boundary, where the resonant transforms into the bound state, which continues until B.z. boundary to reach energy $E = W$[§]. The lines of actual peaks' energies corresponding to constant actual widths are shown in Fig. 3. In the inset we can see the values of W/t needed to obtain the actual peaks at the band boundary (lower curve) and on the boundary between the resonant and quasiresonant states — upper curve (with peaks very close to the line "4t" in the main figure).

3.2. s-wave

Figure 4 is analogous to Fig. 1 with the same denotations but concerns $\langle s_0|G_0|s_0\rangle$, i.e., pure *s*-wave state, connected only with on-site U attraction (without the admixture of extended, W-dependent part). The resonant state's $\mathcal{T}^+$ matrix for $U/t = -7.3$ is very narrow and peaked at the band boundary. The quasiresonant state for $U/t = -4$ is much wider but also peaked at the band boundary. That is the largest difference with the *d*-wave case — *s*-wave U-connected resonances do not move inside the band.

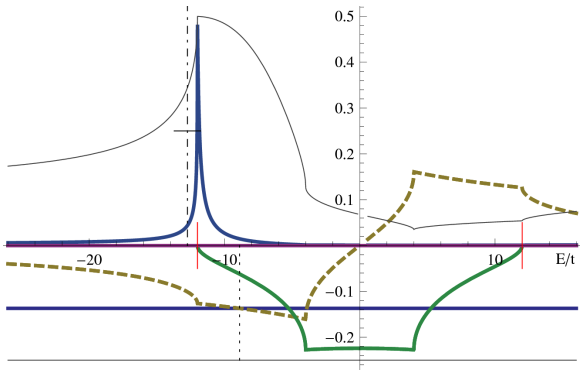

Fig. 4. *s*-wave, $\mathcal{T}$-matrices and t/U values for $U/t = -7$ (narrower) and -4 with Re and Im of $\langle s_0|G_0|s_0\rangle$. The rest of denotations as in Fig. 1.

4. Conclusions

In the paper the two-particle $\mathcal{T}^+$-matrices are calculated for tUW model in the empty lattice limit. The behavior of resonant states connected with the peak of $\mathcal{T}^+$-matrix was examined within symmetry channels (*s* and *d*) and compared with the known approximate formula. With decreasing Coulomb interactions the relative height of the peak diminishes but it remains well defined even for interactions so weak that the resonant state Eq. (27) is not fulfilled. In the same time the peaks become wider and they travel inside the band in the case of *d*-wave (and other W controlled pairings, like *p*-wave and, partly, extended *s*-wave) or stay "glued" at the band

[§]The author thanks R. Micnas for pointing out that property.

boundary — case of pure s-wave. The approximate formulae are correct only close to band boundaries; for small $|\boldsymbol{K}|$ "the correctness range" is wider.

References

[1] D.J. Van Harlingen, *Rev. Mod. Phys.* **67**, 515 (1995).

[2] Y.J. Uemura, L.P. Le, G.M. Luke, B.J. Sternlieb, W.D. Wu, J.H. Brewer, T.M. Riseman, C.L. Seaman, M.B. Maple, M. Ishikawa, D.G. Hinks, J.D. Jorgensen, G. Saito, H. Yamochi, *Phys. Rev. Lett.* **66**, 2665 (1991).

[3] O.K. Andersen, W. Klose, H. Nohl, *Phys. Rev. B* **17**, 1209 (1978).

[4] A.P. Mackenzie, Y. Maeno, *Rev. Mod. Phys.* **75**, 657 (2003).

[5] M. Sigrist, K. Ueda, *Rev. Mod. Phys.* **63**, 239 (1991).

[6] P. Starowicz, C. Liu, R. Khasanov, T. Kondo, G. Samolyuk, D. Gardenghi, Y. Lee, T. Ohta, B. Harmon, P. Canfield, S. Bud'ko, E. Rotenberg, A. Kaminski, *Phys. Rev. B* **77**, 134520 (2008).

[7] M.Z. Hasan, C.L. Kane, *Rev. Mod. Phys.* **82**, 3045 (2010).

[8] T. Saito, S. Onari, H. Kontani, *Phys. Rev. B* **88**, 045115 (2013).

[9] C. Liu, T. Kondo, Ni Ni, A.D. Palczewski, A. Bostwick, G.D. Samolyuk, R. Khasanov, M. Shi, E. Rotenberg, S.L. Bud'ko, P.C. Canfield, A. Kaminski, *Phys. Rev. Lett.* **102**, 167004 (2009).

[10] S. Salem-Sugui, Jr., J. Mosqueira, A.D. Alvarenga, *Phys. Rev. B* **80**, 094520 (2009).

[11] R. Micnas, *Phys. Rev. B* **76**, 184507 (2007).

[12] B. Tobijaszewska, R. Micnas, *Phys. Status Solidi B* **243**, 159 (2006).

[13] Chih-Chun Chien, Hao Guo, Yan He, K. Levin, *Phys. Rev. A* **81**, 023622 (2010).

[14] M. Bak, R. Micnas, *J. Phys. Condens. Matter* **10**, 9029 (1998).

[15] F. Pistolesi, P. Nozieres, *Phys. Rev. B* **66**, 054501 (2002).

[16] M. Randeria, Ji-Min Duan, Lih-Yir Shieh, *Phys. Rev. Lett.* **62**, 981 (1989).

[17] S. Robaszkiewicz, R. Micnas, J. Ranninger, *Phys. Rev. B* **36**, 180 (1987).

[18] R. Micnas, J. Ranninger, S. Robaszkiewicz, *Rev. Mod. Phys.* **62**, 113 (1990).

[19] T. Kostyrko, R. Micnas, *Acta Phys. Pol. A* **83**, 837 (1993).

[20] R. Friedberg, T.D. Lee, H.C. Ren, *Phys. Rev. B* **50**, 10190 (1994).

[21] A.S. Blaer, H.C. Ren, O. Tchernyshyov, *Phys. Rev. B* **55**, 6035 (1997).

[22] M. Bak, R. Micnas, *Mol. Phys. Rep.* **24**, 236 (1999); arXiv:cond-mat/9909089, [cond-mat.supr-con].

[23] M. Bak, *Acta Phys. Pol. A* **121**, 808 (2012).

[24] M. Bak, *Acta Phys. Pol A* **111**, 781 (2007).

[25] M. Bak, *Phys. Status Solidi B* **244**, 2421 (2007).

[26] M. Bak, R. Micnas, *Acta Phys. Pol. A* **97**, 209 (2000).

[27] M. Bak, *Phys. Status Solidi B* **242**, 420 (2005).

[28] H.Q. Lin, *Phys. Rev. B* **44**, 4674 (1991).

[29] A.G. Petukhov, J. Galan, J.A. Verges, *Phys. Rev. B* **46**, 6212 (1992).

[30] M.Y. Kagan, T.M. Rice, *J. Phys. Condens. Matter* **6**, 3771 (1994).

[31] S. Basu, A. Callan-Jones, R.J. Gooding, *Phys. Rev. B* **66**, 144507 (2002).

[32] C.Y. Kadolkar, S. Basu, *Phys. Rev. B* **73**, 104501 (2006).

[33] F.J. Dyson, *Phys. Rev.* **102**, 1217 (1956).

[34] M. Wortis, *Phys. Rev.* **132**, 85 (1963).

[35] G.S. Joyce, *J. Phys. A Gen. Phys.* **5**, L65 (1972).

[36] M. Valiente, D. Petrosyan, *J. Phys. B At. Mol. Opt. Phys.* **41**, 161002 (2008).

[37] J. Javanainen, O. Odong, J.C. Sanders, *Phys. Rev. A* **81**, 043609 (2010).

[38] G.F. Koster, J.C. Slater, *Phys. Rev.* **95**, 1167 (1954).

[39] G.F. Koster, J.C. Slater, *Phys. Rev.* **96**, 1208 (1954).

[40] J. Callaway, *J. Math. Phys.* **5**, 783 (1964).

[41] H. Callen, *Phys. Rev. B* **6**, 1010 (1972).

[42] M. Bak, *Acta Phys. Pol. A* **121**, 808 (2012).

[43] T. Wolfram, J. Callaway, *Phys. Rev.* **130**, 2207 (1963).